Photoinduced Processes in Heterogeneous Gas−Solid Systems. Temperature Dependence (100−600 K) and Modeling of a Surface Chemical Reaction on Zirconia that Triggers Photophysical Events in the Solid

A. V. Emeline,*,† S. Polikhova,‡ N. Andreev,‡ V. Ryabchuk,‡ and N. Serpone*,†

Department of Chemistry & Biochemistry, Concordia University, 1455 de Maisonneuve Blvd. West, Montreal, Quebec, Canada H3G 1M8, and Department of Photonics, Institute of Physics, State University of St. Petersburg, St. Petersburg, Russia

Received: December 31, 2001

We report studies on photoinduced processes that take place in gas−solid heterogeneous systems. In particular, we examine the chemical reaction (i.e., chemical relaxation pathway) between hydrogen (or methane) and the surface of ZrO_2 particles which occurs after the solid was preirradiated (vacuo or oxygen) and the intrinsic phosphorescence from zirconia had terminated. Introduction of H_2 yields an after-glow (light pulse referred as photoinduced chesorluminescence, PhICL) that is caused by chemical interaction between the photoactivated surface of the photocatalyst and the H-containing molecules in the heterogeneous gas−solid system. Unlike hydrogen, methane does not yield a detectable PhICL emission. The PhICL emission for hydrogen decays via biphasic kinetics ($\tau_1 = 0.9$ s and $\tau_2 = 10$ s; ambient temperature). Reactions were also investigated in the temperature range of 75−600 K. For a nonpreirradiated surface, the H-containing molecules physisorb with binding energy $E_{phys} = 33$ kJ mol^{-1} (0.34 eV) for H_2 and 52 kJ mol^{-1} (0.54 eV) for CH_4. After preirradiation of ZrO_2, the molecules chemisorb dissociatively yielding free radicals ($H^\bullet$ for H_2, and $CH_3^\bullet$ for methane, the other $H^\bullet$ is trapped) through an activated process; activation energies $E_a = 30$ kJ mol^{-1} (0.31 eV) for H_2 and 32 kJ mol^{-1} (0.33 eV) for CH_4 if the process occurs by a Langmuir-type pathway; if the process occurs by an Eley-Rideal mechanism, $E_a = 41$ kJ mol^{-1} (0.43 eV) for H_2 and 46 kJ mol^{-1} (0.48 eV) for CH_4. The data were modeled through a sequence of differential equations. A mechanism is proposed that involves shallow traps and deep energy traps for electrons to explain the photophysical events triggered by the surface chemical reaction. In essence, surface chemical reactions cause the release of the energy stored during the preirradiation stage of the solid. This results in photoinduced formation of metastable defects in the solid (e.g., $O_s^{-\bullet}$) together with deep electron traps (**F** centers) that lead to both chemical and physical relaxation of the system.

Introduction

Absorption of actinic light by a heterogeneous system creates a new thermodynamic system with flow of free energy that drastically changes its chemical and physical behavior. The energy flow of the light absorbed by the solid creates a new thermodynamic state of the solid. If the solid is not a degenerate semiconductor (typical of photocatalysts), the next expression is true in the dark (E_G, band gap energy):

$$[e^-][h^+] = n_i^2 = N_C N_V e^{-(E_G/\kappa T)} \quad (1)$$

where N_C and N_V denote the densities of electronic states in the conduction band and valence band, respectively. The concentration of electrons, $[e^-]$, and holes, $[h^+]$, depends on the position of the Fermi level. Under irradiation, the Fermi level of the catalyst splits into two quasi-Fermi levels: one for electrons (F_e) and the other for holes (F_h), provided that the relaxation times of momentum and energy are smaller than the lifetime of the charge carriers in the corresponding bands. Under irradiation the expression can be written as

$$[e^-][h^+] = n_i^2 = e^{(F_e - F_h/\kappa T)} = N_C N_V e^{-(E_G - \Delta F/\kappa T)} \quad (2)$$

where $\Delta F = F_e - F_h$. Clearly, a catalyst under irradiation behaves differently with an apparent band gap given by $E_G - \Delta F$; this leads to changes in the concentration of free charge carriers. As a result, wide band gap solids display increased activity in surface chemical processes involving surface charge carriers.[1−5]

The energy difference between the two quasi-Fermi levels, ΔF, depends on the intensity of irradiation. Accordingly, different states result that behave as different catalysts at different light intensities. At the higher light intensities the concentrations of electrons and holes (i.e., of the reactive centers) are also greater. The extent that Fermi level splitting occurs only under irradiation suggests that this photoinduced state of the system is unstable and has a tendency to relax to its lower energy state, which in the ideal case is to its initial ground state.

Two general pathways can be distinguished for the relaxation of photoinduced states: chemical and physical, which tend to compete with one another.[5,6] The chemical pathway is represented by surface photochemical reactions that produce lower energy products, such as photoadsorbed molecules or products of oxidation. However, the complete relaxation of the solid occurs through a chemical pathway *only* for true photocatalytic

* To whom correspondence should be addressed. Fax: +1 (514) 848-2868. E-mail: serpone@vax2.concordia.ca.
† Concordia University.
‡ State University of St. Petersburg.

10.1021/jp014644k CCC: $22.00
Published on Web 05/21/2002

processes of interfacial electron transfer, provided that the quantum yields of both reduction and oxidation reactions are unity, at least in the very ideal case. Otherwise, physical relaxation competes effectively with chemical relaxation. Some photocatalytic reactions that are not accompanied by electron transfer (e.g., isotope exchange processes) do not lead to system relaxation.

Complete relaxation of the system through a physical pathway occurs because of recombination of free charge carriers in the solid. However, in real solids, the absence of complete recombination through the defects leads to the formation of new photoinduced defects (color centers). These store some of the excess energy compared to the initial state of the solid.[5,7,8] By analogy with quasi-Fermi levels of photogenerated free electrons and holes, the energy distribution of carriers trapped by defects can be described in terms of a quasi-Fermi level for trapped carriers, which differs from the initial position of the Fermi level in a nonirradiated catalyst.

Unlike free carriers, the energy distribution of carriers trapped by deep-energy defects can be frozen in the metastable state after irradiation is halted and will return to its initial state only after additional external stimulations of increased temperature or irradiation of the solid in a corresponding spectral region. Such a transition from the metastable to the initial stable state may be accompanied, for example, by luminescence emission which can characterize the relaxation processes in the system.

We showed earlier[8,9] that competition between chemical and physical relaxation pathways can be presented as

$$r_{ox} + \frac{d[\mathbf{V}]}{dt} = r_{red} + \frac{d[\mathbf{F}]}{dt} \qquad (3)$$

where r_{ox} and r_{red} are the rates of oxidation and reduction reactions taking place at the surface, respectively, and d[V]/dt and d[**F**]/dt are the rates of hole and electron trapping by defect sites such as cation (V_c) and anion (V_a) vacancies, respectively.

Herein, we report our recent studies of photoinduced processes in heterogeneous systems when the chemical reaction (chemical relaxation pathway) triggers physical relaxation processes. The latter manifest themselves, in particular, as a photoinduced chesorluminescence (PhICL) caused by chemical interaction between the photoactivated surface of the photocatalyst and hydrogen-containing molecules in the heterogeneous gas−solid system.[9−12]

Experimental Section

The powdered monoclinic form of the ZrO_2 specimen was of high purity grade ("7−4", IREA, Russia) having a specific surface area of ca. 7 $m^2\ g^{-1}$ (BET method; nitrogen gas). The specimen was pretreated as described earlier [8,12] to remove ubiquitous organic impurities and other adventitious adsorbed molecules. Reproduction of the original state of the specimens between experiments was achieved by heating the samples in an oxygen atmosphere for about 1 h. Experimental errors in the spectral measurements caused by the nonreproducibility of the original state of the specimen are unlikely to exceed ca. ±10%.

Powdered samples were contained in a quartz cell (path length 3 mm; illuminated area, 6 cm^2) connected to a high-vacuum setup equipped with an oil-free pump system. The ultimate gas pressure in the reaction cell was ca. 10^{-7} Pa. A Pirani-type manometer (sensitivity, 18 mV Pa^{-1} for O_2 and 24 mV Pa^{-1} for H_2) measured the gas pressures. Monitoring of the chemical composition of the gas phase, partial pressure of the gases, and desorption products were carried out with a mass spectrometer (model MX7301) connected to the reactor.

Irradiation of the solid specimens was achieved with a 120 W high-pressure Hg lamp (MELZ, DRK-120; photon flux at wavelengths below 250 nm was $\sim 10^{15}$ photons $cm^{-2}\ s^{-1}$). The power density at wavelengths below 400 nm (6 mW cm^{-2}) was measured through a water filter using a thermoelement (IOFI; sensitivity, 1.5 V per Watt). The luminescence was recorded with a KSVU-12 spectral setup (LOMO) adapted to record luminescence emission of solid powders in vacuo.

Two thermoprogrammed devices were used to measure the thermoluminescence, the thermodesorption, and the temperature dependencies of the postirradiation adsorption of gases on the preirradiated ZrO_2 surface. One device was operated in the temperature range of 100−300 K with the rate of linear temperature increase (α) set at 0.1 K s^{-1}; the working temperature range of the second device was 300−800 K with α set at 0.3 K s^{-1}. The two devices maintained the temperature constant to within ca. ±5 K.

Results and Discussion

Chemisorption of hydrogen-containing molecules, for example H_2, H_2O, hydrocarbons (RH), and alcohols (ROH) on preirradiated metal-oxide surfaces emit light following interaction of these molecules with photogenerated surface active centers. The effect, which we denote as *photoinduced chesorluminescence* (PhICL), was first detected by Andreev and Kotel′nikov.[10] In their original study, they examined the fate of H_2O, H_2, and CH_4 on prephotoactivated surfaces of Al_2O_3 and MgO.[10,13] In our previous report,[12] we showed that this effect is also typical for the adsorption of molecular hydrogen on preirradiated powdered ZrO_2. The light pulse from the PhICL effect follows biexponential decay kinetics with the longer component corresponding to the phosphorescence decay process. As well, PhICL emits photons in a broad spectral range with the maximum at ca. 490 nm. As expected, the PhICL spectrum corresponds to the phosphorescence and thermostimulated luminescence (TSL) spectra of ZrO_2. In turn, this infers similar mechanisms of the emission process, namely, trapping of electrons by such deep traps as anion vacancies, V_a.

The PhICl phenomenon is another example of the interconnection between chemical and physical relaxation pathways in a heterogeneous system. We now describe the results of extended experimental studies of the PhICL effect caused by adsorption of H_2 on a preirradiated surface of ZrO_2. The data are compared with processes of adsorption of another H-containing molecule, namely, methane.

Kinetics of the PhICL Effect. The kinetics of decay of the PhICL emission following the addition of hydrogen gas (initial concentration, ca. 100 Pa) on the surface of ZrO_2 preirradiated for 15 min in vacuo are illustrated in Figure 1. The kinetics are approximated by the sum of two exponential terms (biphasic decay) yielding $\tau_1 = 0.9$ s and $\tau_2 = 10$ s. To eliminate the influence of ZrO_2 phosphorescence on the kinetics of PhICL, the hydrogen gas was introduced and adsorption achieved about 10 min after the preirradiation period when the intrinsic zirconia afterglow (i.e., emission) was nearly ended.

Influence of the PhICL Effect on the Luminescence of Zirconia. Zirconium dioxide displays different types of luminescence (X-ray induced and photoinduced phosphorescence and thermoluminescence of a preirradiated sample) with a broad emission band located around 475 nm (see insert to Figure 1). The emission band is a complex one formed by overlapping of at least two single bands,[8,12] which corresponds to different types

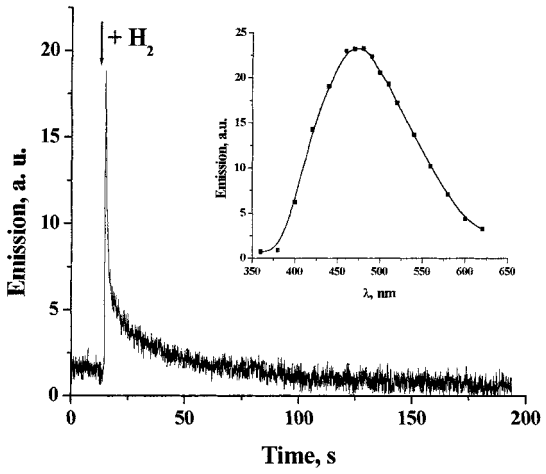

Figure 1. Decay kinetics of the PhICL emission (at $\lambda = 490$ nm) induced by hydrogen adsorption after preirradiation of zirconia in vacuo for 15 min. The insert depicts the PhICL emission spectrum.

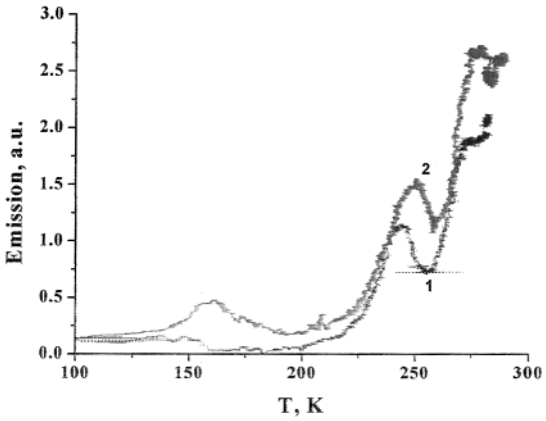

Figure 2. Thermal dependence from 100 to 300 K of the thermostimulated luminescence (TSL) after preirradiation of ZrO_2 at ambient temperature in vacuo for 15 min: (1) reference, (2) after the postirradiation adsorption of hydrogen.

of deep-energy electron traps. One of these traps is identified as anion vacancies, V_a , to give an **F** center:[8,12,14,15]

$$V_a + e^- \rightarrow \mathbf{F} + h\nu \qquad (4)$$

Because the spectrum of the PhICL emission corresponds to the spectra of photo and thermo luminescence and phosphorescence[8,12] and the origins of the various types of emissions are rather similar (see eq 4), we expect to observe the influence of hydrogen adsorption on a preirradiated zirconia surface on the PhICL effect and on the luminescence of ZrO_2.

Figures 2 and 3 illustrate the thermal glow from preexcited ZrO_2 in vacuo recorded at $\lambda = 490$ nm in two temperature regions: from 100 K to ambient temperature (Figure 2) and from ambient temperature to 600 K (Figure 3). As evidenced from these results, zirconia possesses a broad energy distribution of electron traps. Hydrogen adsorption has suppressed the first band whose maximum appears at $T = 350$ K in the thermal glow of zirconia (Figure 3) when hydrogen was allowed to be adsorbed at ambient temperature, whereas it caused an increase of the thermal glow in the low temperature range. Accordingly, we infer that transfer of energy released in the chemical steps from the surface to the bulk leads to electron detrapping from deep traps. If adsorption of hydrogen were allowed to occur at low temperature (e.g., at $T = 200$ K) detrapped electrons can be retrapped by the shallow traps, which leads to an increase in

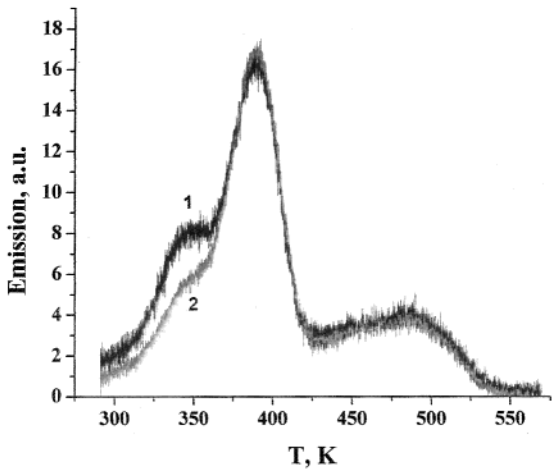

Figure 3. Thermal dependence from 300 to 600 K of TSL after preirradiation of ziconia at ambient temperature in vacuo for 15 min: (1) reference, (2) after the post-irradiation adsorption of hydrogen.

the low-temperature thermal glow. At ambient temperatures, these shallow traps are completely thermoionized. The following sequence of steps I−V summarize these observations:

$$H_2 + ZrO_2^* \rightarrow\rightarrow (ZrO_2 \text{ - - } H_2)^* \rightarrow\rightarrow\rightarrow (ZrO_2 - H_2) + \Delta E \quad \text{(I)}$$

$$D^- + \Delta E \rightarrow D + e^- \qquad \text{(II)}$$

$$e^- + T_{sh} \rightarrow T_{sh}^- \qquad \text{(III)}$$

$$T_{sh}^- \rightarrow T_{sh} + e^- \qquad \text{(IV)}$$

$$e^- + V_a \rightarrow \mathbf{F} + h\nu \qquad \text{(V)}$$

where, step I describes the general chemical processes beginning from the postirradiation adsorption of hydrogen that causes the release of energy ΔE, followed by energy transfer to the bulk defects D^- in zirconia; this in turn induces the ionization of D^- and the formation of free electrons (step II). Subsequently, these electrons can be trapped either by the shallow traps T_{sh} (step III) or by the deep energy emission centers V_a (step V) to yield the **F** color centers. Steps III and V compete with each other. At low temperature, when the process of detrapping (step IV) from the shallow traps is completely shut down and most of the electrons remain trapped in the shallow traps, the emission becomes very weak. However, at higher temperatures, the efficiency of the detrapping of electrons increases, and electron relaxation to the deep energy defects then becomes more effective as reflected by the growth of the emission intensity. In other words, chemical processes trigger the photophysical processes of the system's relaxation.

Temperature Dependencies of the Kinetic Parameters of PhICL and Postirradiation Adsorption of Hydrogen. A decrease in temperature leads to a decrease of the PhICL emission intensity. Two possible factors explain this observation. As reported earlier,[12] the first is connected to the notion that the longer-lived component of the PhICL emission is due to phosphorescence, for which the electrons generated as a result of a surface chemical reaction are trapped in shallow energy levels (traps) in ZrO_2 before they get trapped by deeper-energy emission centers (eq 4). In this regard, the lower the temperature is, the greater the number of electrons is that are trapped by the shallow defects and that cannot be thermally released (i.e., the

defects cannot be thermally ionized). Accordingly, these electrons cannot participate in the physical process of electron trapping by the emission centers. Thus, the total PhICL intensity decreases at the lower temperatures.

The second factor is that dissociative adsorption of hydrogen (for H-containing donor molecules) on surface-active hole centers is an activated process (see below). Thus, it must overcome an activation barrier. Consequently, at the lower temperatures, a smaller number of molecules initiate the chemical sequence, which results in a PhICL effect that causes a decrease of the PhICL emission intensity. As observed earlier,[12] at liquid-nitrogen temperatures, most (but not all) surface-active centers do not react with hydrogen. Nonetheless, some of these centers do infer an energetic heterogeneity of the photogenerated surface-active centers.

Figure 4a reports the temperature dependence of the observed amplitude and integrated (i.e., total number of photons emitted) PhICL emission induced by the post-irradiation adsorption of hydrogen, whereas Figure 4b,c summarizes the relevant temperature dependencies of the preexponential factors A_1 and A_2, as well as of the decay times τ_1 and τ_2. As evidenced by the experimental data presented in Figures 2 and 3, both factors noted above play a role in the observed phenomenon.

Figure 5 displays the temperature dependence of the evolution of hydrogen pressure over the nonirradiated and the preirradiated zirconia surface. In the case of the nonirradiated surface, the pressure evolution is dictated only by the dark physical adsorption/desorption processes and by the temperature-dependent increase in pressure. By contrast, at the preirradiated surface, the hydrogen molecules also interact chemically with the photogenerated surface-active hole centers, causing a different pressure behavior.

The difference in the pressure evolution begins around 180 K when most centers become active enough to overcome the activation barrier. Thus, the temperature evolution of the PhICL effect and the postirradiation adsorption of hydrogen depend on the activation energy of dissociative adsorption of the hydrogen molecules on the photogenerated active centers. Assuming that hydrogen adsorption on the nonpreirradiated surface is a physisorption phenomenon and that desorption is dictated by the thermal cleavage of the physisorption "bonds", it then becomes possible to estimate the activation energy of dissociative adsorption of hydrogen on the preirradiated surface. In a simple model of desorption of physisorbed hydrogen from the homogeneous surface, one has

$$H_{2(phys)} \xrightarrow{k_{des}} H_{2(gas)} \tag{5}$$

$$\frac{d[H_{2gas}]_1}{dt} = k_{des}[H_{2phys}] \tag{6a}$$

and

$$\frac{d[H_{2gas}]_1}{dt} = k^{\circ}_{des}[H_{2phys}]e^{-E_{phys}/\kappa T} \tag{6b}$$

The experimental data yield the binding energy of physisorption $E_{phys} = 33$ kJ mol^{-1} (0.34 eV). Consequently, in the case of a preirradiated surface, dissociative adsorption becomes an additional process that influences the pressure evolution.

We consider two different pathways to describe the dissociative interaction of hydrogen molecules with photoinduced surface-active centers. The first is the well-known Langmuir−Hinshelwood (LH) type mechanism, whereby physisorbed molecules react with the $O_s^{-\bullet}$ centers. The other is the Eley−Rideal (ER) mechanism, whereby the predesorbed molecules attack the surface-active centers from the gas phase. Accordingly, we have for the LH path

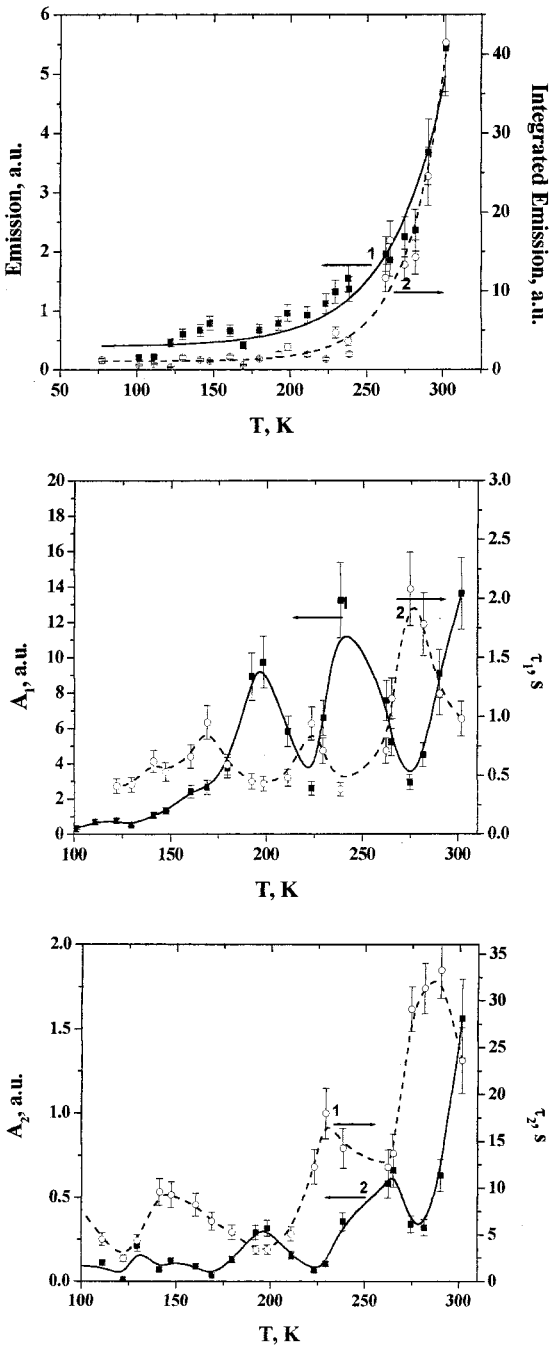

Figure 4. (a) Temperature dependence from 75 to 300 K of the observed emission amplitude (1) and integrated emission (2) of the PhICL luminescence induced by the postirradiation adsorption of hydrogen. (b) Temperature dependence from 100 to 300 K of the preexponential factor A_1 (1) and the exponential decay time τ_1 (2) of the first term of the biphasic decay kinetics of the PhICL emission. (c) Temperature dependence from 100 to 300 K of the preexponential factor A_2 (1) and the exponential decay time τ_2 (2) of the second term of the biphasic decay kinetics of the PhICL emission.

$$\text{(LH)} \qquad H_{2(phys)} + O_s^{-\bullet} \xrightarrow{k_{ads}} OH^- + H^{\bullet} \tag{7a}$$

and for the ER pathway

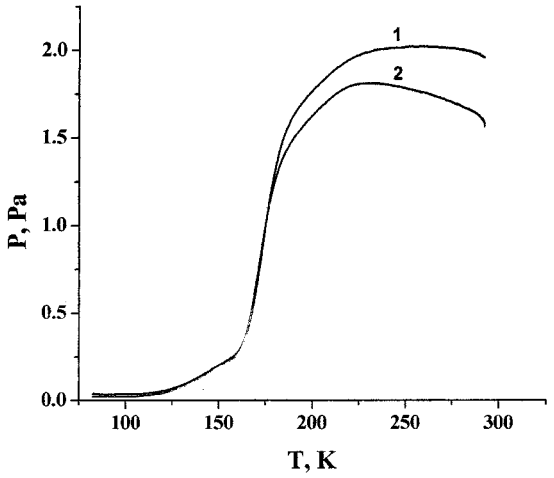

Figure 5. Temperature dependence from 75 to 300 K of the pressure evolution of hydrogen over nonirradiated (1) and preirradiated zirconia (2) in vacuo for 15 min.

$$\text{(ER)} \qquad H_{2(gas)} + O_s^{-\bullet} \xrightarrow{k'_{ads}} OH^- + H^\bullet \qquad (7b)$$

from which we obtain

$$\frac{d[H_{2gas}]_2}{dt} = k_{des}[H_{2phys}] - k_{ads}[H_{2phys}][O_s^{-\bullet}] \qquad (8a)$$

and

$$\frac{d[H_{2gas}]_2}{dt} = k_{des}[H_{2phys}] - k'_{ads}[H_{2gas}][O_s^{-\bullet}] \qquad (8b)$$

respectively. As a result, the difference in pressure evolution will be given by eq 9:

$$\frac{d(\Delta[H_{2gas}])}{dt} = \frac{d[H_{2gas}]_2}{dt} - \frac{d[H_{2gas}]_1}{dt} \qquad (9)$$

Accordingly, for the LH pathway, this change in pressure is given by eq 10:

$$\frac{d(\Delta[H_{2gas}])}{dt} = -k_{ads}[H_{2phys}][O_s^{-\bullet}] \qquad (10a)$$

or

$$\frac{d(\Delta[H_{2gas}])}{dt} = -k^\circ_{ads}[H_{2phys}][O_s^{-\bullet}]e^{-E_a/\kappa T} \qquad (10b)$$

The corresponding change in pressure for the ER pathway is given by eq 11:

$$\frac{d(\Delta[H_{2gas}])}{dt} = -k'_{ads}[H_{2gas}][O_s^{-\bullet}] \qquad (11a)$$

or

$$\frac{d(\Delta[H_{2gas}])}{dt} = -k'^\circ_{ads}[H_{2gas}][O_s^{-\bullet}]e^{-E'_a/\kappa T} \qquad (11b)$$

Taking into consideration that $dt = \alpha\, dT$ and that $[H_{2gas}] = P/\kappa T$, then from the experimental pressure evolution data and from $d(\Delta P)/\alpha\, dT$ (Figure 5) the effective activation energy of dissociative adsorption of hydrogen is $E_a = 30$ kJ mol^{-1} (0.31 eV) for the LH mechanism and 41 kJ mol^{-1} (0.43 eV) for the ER pathway. In the latter case, one should take into account that k'°_{ads} will be given by

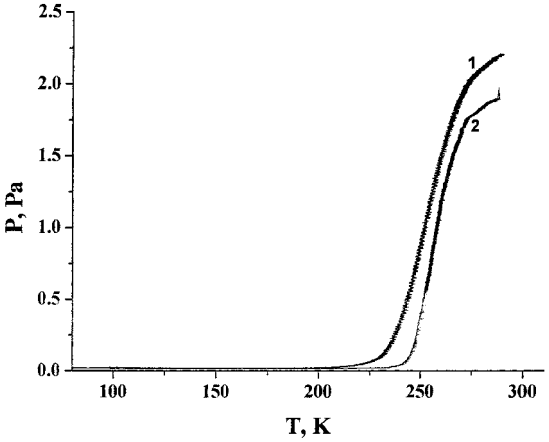

Figure 6. Temperature dependence from 75 to 300 K of the pressure evolution of methane over nonirradiated zirconia (1) and preirradiated zirconia (2) in vacuo for 15 min.

$$k'^\circ_{ads} = \frac{1}{4}\sigma v(T) = \frac{1}{4}\sigma\left(\frac{8RT}{\pi M}\right)^{1/2} \qquad (12)$$

where σ (ca. 10^{-20} m^2) is the cross-section of the chemical interaction between the surface-active centers and the gas molecules, $v(T)$ is the average velocity of the molecules in the gas phase at a given temperature T, R is the gas constant, and M is the molar mass of the gas molecule. A similar behavior was observed for the postirradiation adsorption of methane (Figure 6). We estimated $E_{phys} = 52$ kJ mol^{-1} (0.54 eV) and $E_a = 32$ kJ mol^{-1} (0.33 eV) for the LH pathway and $E_a = 46$ kJ mol^{-1} (0.48 eV) for the ER mechanism.

We infer that the thermal evolution of the gas pressure depends on the thermal behavior of the adsorption of molecules on photogenerated surface-active centers, which is dictated by the magnitude of the activation barrier. The similar activation energies of dissociation for hydrogen and methane suggest that the major feature of the processes is the thermal activation of the surface-active centers. A similar behavior explains the decay of the quantum yields of photoadsorption of gases at low temperatures in gas/solid heterogeneous systems containing TiO_2 and ZnO.[16,17]

Introducing hydrogen at a temperature $T = 200$ K leads to an increase in the thermal glow in the temperature range of 200−300 K (see Figure 2, curve 2), caused by the thermoionization of the shallow electron traps that were initially occupied at 200 K. Accordingly, those electrons that are trapped by the shallow defects cannot be trapped by the emission centers, thus resulting in a weaker PhICL emission intensity (curve 1, Figure 2). Moreover, the thermal behavior of the PhICL parameters (amplitudes and decay times; Figure 4) correlates with the thermostimulated luminescence of ZrO_2 (thermal glow; Figure 2). Indeed, the maxima of the temperature dependence of the PhICL luminescence intensity correspond to the temperature range of the minima of thermal glow, whereas the maxima of the decay times correlate with the maxima of thermal glow, which again indicates the important role played by the shallow traps in the PhICL emission.

Dependencies of the Kinetics of the PhICL Effect on the Time of Preirradiation of ZrO_2 and on the Initial Pressure of Hydrogen. Both exponential factors remain constant at

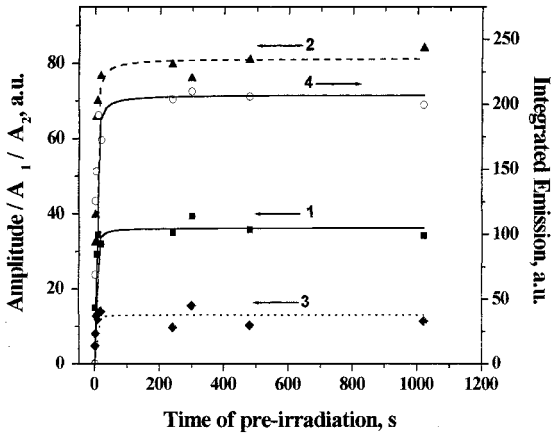

Figure 7. Temporal dependencies of the emission amplitude (1), integrated emission (2), and preexponential factors A_1 and A_2 (3 and 4) of the PhICL emission on the time of preirradiation of zirconia.

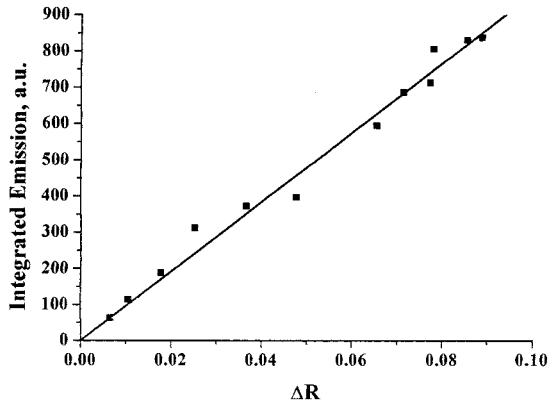

Figure 8. Dependence of the integrated emission of the PhICL luminescence on the absorption of photoinduced color centers.

various exposure times of preirradiation, whereas the experimental amplitude, the two preexponential factors, and the total number of photons emitted for the given time increase with increasing time of preirradiation exposure (Figure 7). The increase of the PhICL amplitude and the integrated number of emitted photons correlate with the absorption growth of the photoinduced color centers at $\lambda = 400$ nm (Figure 8), which scales with the absorption of light (ΔR) by the surface $O_s^{-\bullet}$ centers for hydrogen adsorption.

Preexponential factors of the PhICL luminescence, the experimental emission amplitude, and the integrated number of emitted photons also increase with increasing hydrogen pressure in a sub-linear manner until saturation (Figure 9a). Moreover, the exponential decay times also depend on the hydrogen pressure as evidenced from the data illustrated in Figure 9b. The higher the hydrogen pressure is, the shorter the decay times are. Clearly, the PhICL behavior is not "symmetrical" with respect to the initial concentrations of reagents, namely, the hydrogen pressure and the surface concentration of photogenerated surface-active hole centers. That is, the dependencies of the PhICL parameters on the concentration of surface-active hole centers and on hydrogen pressure display different characteristics.

The "ultimate adsorption capacity" (ΔP_∞) of zirconia with respect to hydrogen molecules depends on the initial pressure, as well as on the parameters of the biexponential approximation of the adsorption kinetics (Figure 10). The adsorption capacity was estimated as the sum of the limits of changes in pressure at very long times ($t \rightarrow \infty$) in a set of adsorption cycles, new

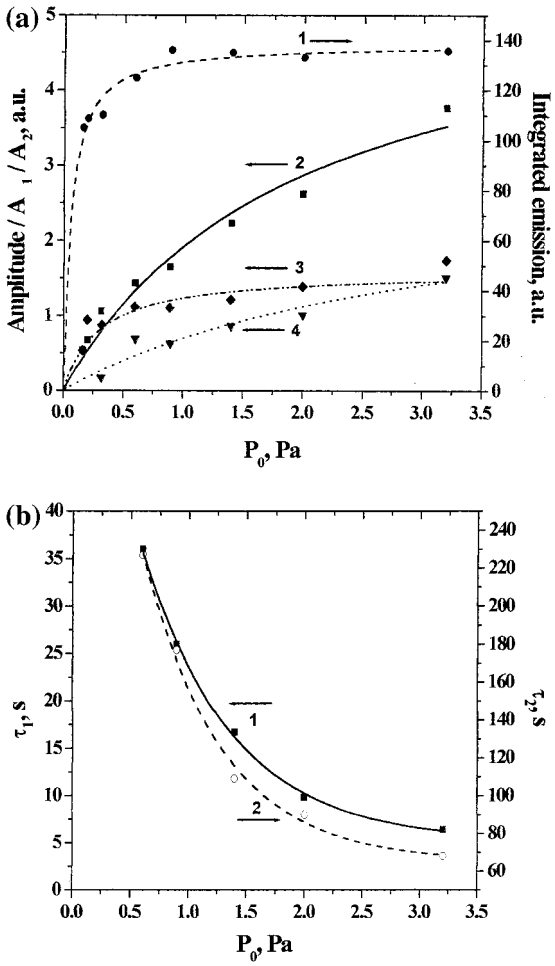

Figure 9. (a) Dependencies of the integrated emission (1), emission amplitude (2), and preexponential factors A_1 and A_2 (3 and 4) of the PhICL emission on the initial hydrogen pressure. (b) Dependencies of the exponential decay times of the PhICL emission on the initial hydrogen pressure.

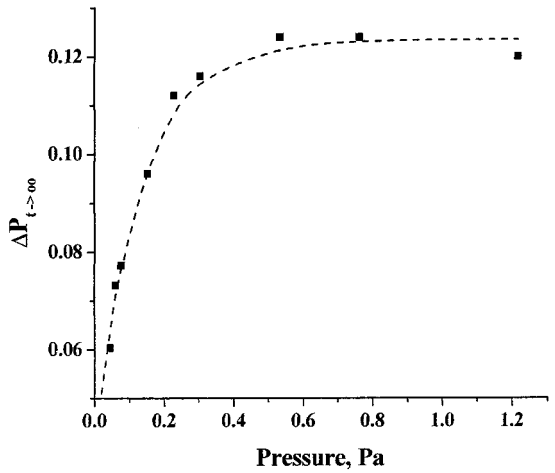

Figure 10. Experimental dependence of the ultimate adsorption capacity of zirconia ($\Delta P_{(t\rightarrow\infty)}$) on the initial hydrogen pressure.

sample of gas at a given initial pressure, until the changes in gas pressure were no longer detectable:

$$\Delta P_{(t\rightarrow\infty)} = \sum_i \Delta P_{i(t\rightarrow\infty)} \qquad (13)$$

where $\Delta P_{i(t\rightarrow\infty)}$ is the adsorption capacity at infinite time for the ith adsorption cycle and $\Delta P_{(t\rightarrow\infty)}$ is the ultimate adsorption

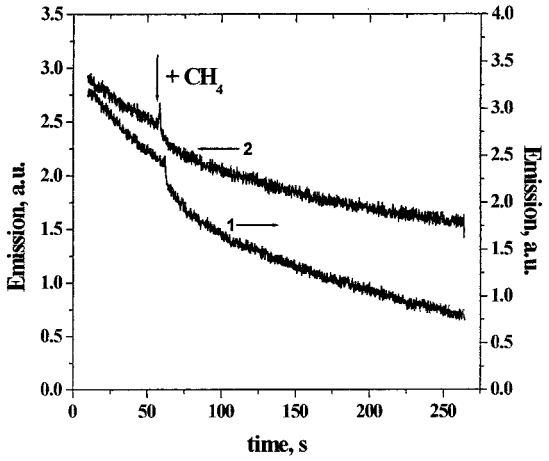

Figure 11. Decay kinetics of the phosphorescence of zirconia after preirradiation in vacuo for 15 min and admittance of methane: (1) preirradiation of zirconia in vacuo, (2) preirradiation of zirconia in an oxygen atmosphere.

capacity of zirconia, which corresponds to the maximal possible surface coverage by adsorbed molecules at a given pressure when changes in pressure are no longer observed. Accordingly, we infer that secondary processes induced by adsorption of hydrogen influence the number of photoinduced adsorption centers. It is reasonable to assume that these involve physical as well as chemical steps in the processes (see section below on simulations).

Introduction of other H-containing donor molecules, such as methane, on a preirradiated zirconia surface does not lead to detectable PhICL emission, unless the metal-oxide specimen has been preirradiated in an oxygen atmosphere. In the latter case, only short, relatively weak light pulses of the PhICL emission were observed (see Figure 11). This suggests that during the secondary chemical steps intermediates effectively trap the free or weakly bound electrons, thereby preventing their being trapped by emission centers (step V above). Possible candidates for such intermediates are the $CH_3^\bullet$ radicals formed by dissociative adsorption of methane on $O_s^{-\bullet}$ surface-active centers. Thus

$$CH_4 + O_s^{-\bullet} \rightarrow OH^- + CH_3^\bullet \quad (14)$$

$$CH_3^\bullet + e^- \rightarrow CH_3^- \quad (15)$$

A similar effect was observed in our previous PhICL studies on a spinel specimen.[11] The above notwithstanding, another hydrocarbon molecule, namely, ethane, does induce PhICL emission on zirconia. Accordingly, we deduce that the chemical steps following the post-irradiation adsorption of the H-containing molecules are different. Regrettably, the current available data do not permit us to speculate on the nature of these steps.

Simulations and Possible Models of Postirradiation Adsorption of Hydrogen and the PhICL Luminescence. We now describe the results of modeling simulations of the dependencies noted above. We consider reasonable assumptions and suggest possible mechanisms of the PhICL effect. Also reported are the results of numerical solutions to the corresponding sets of differential equations that will afford a comparison of the calculated results with those obtained experimentally. This will permit some inferences to be made about the nature of the PhICL effect.

The first step of the PhICL process is well established to be dissociative adsorption of either hydrogen or methane on the surface-active hole centers, $O_S^{-\bullet}$, as given by stage i below:[18,19]

$$H_2 + O_S^{-\bullet} \rightarrow OH^- + H^\bullet \quad (i)$$

We denote the rate of this stage as

$$r_i = k_i P[O_s^{-\bullet}] \quad (16)$$

Earlier, Kotel′nikov and co-workers[10,13] proposed that the PhICL luminescence is caused by radiative decay of an excited state of OH^- formed according to stage i. However, as demonstrated in our previous study,[12] this notion finds no role in the H_2-ZrO_2 heterogeneous system. In fact, the mechanism of the PhICL effect corresponds to the pathway of luminescence of ZrO_2 caused by trapping of free electrons by deep intrinsic traps. Consequently, we infer that hydrogen atoms formed in reaction 7 stimulate secondary surface chemical processes that produce free electrons in the solid, which ultimately induce the PhICL emission. One such process is the interaction of hydrogen atoms with low-coordinated surface oxygen anions O^{2-}, a process that was also considered by Che and Tench.[18] Thus

$$H^\bullet + O^{2-} \rightarrow OH^- + e^- \quad (ii)$$

with the corresponding rate given by

$$r_{ii} = k_{ii}[H^\bullet][O^{2-}] \quad (17)$$

Another possibility considered by Basov and co-workers[19] is an interaction between the hydrogen atoms and the photogenerated surface-active hole centers, $O_s^{-\bullet}$, described by stage iii. That is

$$H^\bullet + O_s^{-\bullet} \rightarrow OH^- \quad (iii)$$

for which

$$r_{iii} = k_{iii}[H^\bullet][O_s^{-\bullet}] \quad (18)$$

In this case, the binding energy (ca. 4.5 eV) of the newly formed O−H bond is released and is used for additional excitation of zirconia by energy transfer from the surface to the bulk of the solid. In this regard, it is worth recalling that the red limit of chemically active photoexcitation of zirconia corresponds to a photon energy of about 3 eV.

In our earlier study,[12] we also considered a possible step in which hydrogen atoms (or methyl radicals in the case of methane) recombine on the surface, stage iv

$$H^\bullet + H^\bullet \rightarrow H_2 \quad (iv)$$

from which

$$r_{iv} = k_{iv}[H^\bullet]^2 \quad (19)$$

The process that yields ethane is well-known to involve the recombination of $CH_3^\bullet$ radicals. Radical recombination also releases the binding energy (ca. 4.5 eV), which can lead to additional excitation of solids with the generation of free electrons. The mechanism(s) of this chemical excitation remains rather elusive at present. Nonetheless, among the many possibilities, we consider the ionization of photogenerated deep energy electron defects as evidenced by the experimental data presented in Figure 3, which shows a decrease of the intensity

of thermal glow after the post-irradiation adsorption of hydrogen:

$$\mathbf{F} \rightarrow e^- + V_a \qquad (v)$$

from which

$$r_v = k_v[\mathbf{F}] \qquad (20)$$

Another possibility is excitation of the intrinsic states S (bulk defects or surface states) responsible for the low-energy photoexcitation of zirconia. In the latter case, the generation of free holes is also expected, because photoexcitation of zirconia with low-energy photons also leads to the photogeneration of both electrons and holes. Accordingly

$$S + h\nu' \rightarrow e^- + h^+ \qquad (vi)$$

from which

$$r_{vi} = k_{vi}[S] \qquad (21)$$

The PhICL luminescence (an emission among other types in zirconia) results from the trapping of electrons by deep-energy defects such as anion vacancies, V_a, (stage vii):

$$e^- + V_a \rightarrow \mathbf{F} + h\nu \qquad (vii)$$

for which the emission intensity scales with r_{vii} as given by eq 22:

$$I_{em} \propto r_{vii} = k_{vii}[e^-][V_a] \qquad (22)$$

Note also that electrons can recombine with surface-active hole centers, thereby decreasing their concentration, in competition with the chemical pathway of hydrogen adsorption (stage iii) as is typical for photostimulated adsorption:[9,20]

$$e^- + O_s^{-\bullet} \rightarrow V_c \qquad (viii)$$

yielding the rate

$$r_{viii} = k_{viii}[e^-][O_s^{-\bullet}] \qquad (23)$$

In turn, if utilization of the energy released in chemical stages iii and iv leads to the generation of both electrons and holes, as inferred in stage vi, hole trapping by surface defects such as cation vacancies, V_c, can lead to formation of new surface-active centers for hydrogen chemisorption. Hence

$$h^+ + V_c \rightarrow O_s^{-\bullet} \qquad (ix)$$

and the rate is given by

$$r_{ix} = k_{ix}[h^+][V_c] \qquad (24)$$

In addition, recombination of free holes with electrons trapped in **F**-type centers can lead to a decrease of electron surface defects, which provides an alternative (compare with stage v) explanation for the experimentally observed decrease of the thermal glow from zirconia:

$$h^+ + \mathbf{F} \rightarrow V_a \qquad (x)$$

for which the rate is

$$r_x = k_x[h^+][\mathbf{F}] \qquad (25)$$

Consequently, to infer the most realistic pathway we need to consider several possible scenarios. We do this by comparing the experimental results with those originating from modeling and simulating the behavior of the heterogeneous system, which leads to adsorption of hydrogen and to the PhICL emission.

Simulation and Modeling. In the first instance, to model kinetically the experimentally observed ultimate adsorption capacity of zirconia (see Figure 10), we first considered the simplest mechanism, one that involves only the generated electrons from the interaction of hydrogen atoms with surface lattice oxygen anions (stage ii). The set of corresponding equations needed to evaluate the appropriate kinetic behavior of the system is summarized by the sequence of differential eqs 26−32:

$$dP/dt = -r_i \qquad (26)$$

$$d[O_s^{-\bullet}]/dt = -r_i \qquad (27)$$

$$d[O^{2-}]/dt = -r_{ii} \qquad (28)$$

$$d[e^-]/dt = r_{ii} - r_{vii} \qquad (29)$$

$$d[H^\bullet]/dt = r_i - r_{ii} \qquad (30)$$

$$d[\mathbf{F}]/dt = r_{vii} \qquad (31)$$

$$I_{em} \propto r_{vii} \qquad (32)$$

Simulation of the pathway using this sequence revealed that the ultimate adsorption capacity does not depend on the initial pressure, because it was determined only by the number of photogenerated adsorption centers. Accordingly, the corresponding mechanism is of no consequence in accounting for the adsorption of hydrogen on zirconia. The appropriate simulation will necessitate additional considerations.

We next consider the likelihood that the $O_s^{-\bullet}$ active centers physically decay through recombination with free electrons (stage viii), which may change the ultimate adsorption capacity of the photoadsorbent ZrO_2. This requires that eq 27 be replaced by eq 33

$$d[O_s^{-\bullet}]/dt = -r_i - r_{viii} \qquad (33)$$

and eq 29 be replaced by eq 34

$$d[e^-]/dt = r_{ii} - r_{vii} - r_{viii} \qquad (34)$$

The results of the numerical solution to this modified set of differential equations (namely, eqs 26, 28, and 30−34) show that for this case there does exist a dependence of the ultimate adsorption capacity on the gas pressure. However, because of a negative interrelationship between the rates of chemical and physical decays, the dependence turns out to be somewhat insignificant requiring much larger changes in pressure (by several orders of magnitude) to achieve a level of the difference in ultimate adsorption capacity around 15−20% at various gas pressures. We deduce that the physical decay of the adsorption centers induced by free electrons produced in stage ii is a possible factor that affects the magnitude of the ultimate adsorption capacity. However, it is undoubtedly not the sole factor.

We further consider the chemical reaction between hydrogen atoms and surface-active hole centers (stage iii) as an additional possibility. This process should provide a greater effect on the pressure dependence because the chemical interaction, which changes the number of adsorption centers (stage iii), depends

on the concentration of H• atoms. In turn, the latter hinges on the pressure of hydrogen gas. Inclusion of this inference suggests that the overall process can be described either by the following set of equations (26, 32, 35−38):

$$dP/dt = -r_i \quad (26)$$

$$I_{em} \propto r_{vii} \quad (32)$$

$$d[O_s^{-\bullet}]/dt = -r_i - r_{iii} \quad (35)$$

$$d[e^-]/dt = r_{iii}r_v - r_{vii} \quad (36)$$

$$d[H^\bullet]/dt = r_i - r_{iii} \quad (37)$$

$$d[\mathbf{F}]/dt = r_{vii} - r_v \quad (38)$$

or by the sequence described by eqs 26, 31, 32, 35, 37, and 39; thus

$$dP/dt = -r_i \quad (26)$$

$$d[\mathbf{F}]/dt = r_{vii} \quad (31)$$

$$I_{em} \propto r_{vii} \quad (32)$$

$$d[O_s^{-\bullet}]/dt = -r_i - r_{iii} \quad (35)$$

$$d[H^\bullet]/dt = r_i - r_{iii} \quad (37)$$

$$d[e^-]/dt = r_{iii}r_{vi} - r_{vii} \quad (39)$$

Modeling with these two sets of differential equations shows that at sufficiently high pressures of hydrogen a significant number of H• atoms accumulates on the zirconia surface. This occurs because after the completion of hydrogen adsorption (stage i) there are no more $O_s^{-\bullet}$ centers left to react with H• atoms. Such a situation, however, is distantly removed from actuality because of the very high reactivity of H• atoms. Evidently, there must exist additional pathways for the H• atoms to decay chemically; one such path for example is through stage ii. Note that the physical pathway of recombination of free electrons with $O_s^{-\bullet}$ centers remains valid nonetheless. Consequently, we consider the modified sequence of differential eqs 26, 28, 32, 38, and 40−42:

$$dP/dt = -r_i \quad (26)$$

$$d[O^{2-}]/dt = -r_{ii} \quad (28)$$

$$I_{em} \propto r_{vii} \quad (32)$$

$$d[\mathbf{F}]/dt = r_{vii} - r_v \quad (38)$$

$$d[O_s^{-\bullet}]/dt = -r_i - r_{iii} - r_{viii} \quad (40)$$

$$d[e^-]/dt = r_{iii}r_v + r_{ii} - r_{vii} - r_{viii} \quad (41)$$

$$d[H^\bullet]/dt = r_i - r_{ii} - r_{iii} \quad (42)$$

The results of the numeric solution to this last sequence are illustrated graphically in Figures 12a,b and 13. Note the reasonably good qualitative correspondence between the experimental and simulated pressure dependencies (compare with Figures 9 and 10). The results of the numeric solutions to the above set of corresponding differential equations also infer that the "nonsymmetrical" behavior of the PhICL parameters on pressure and on the concentration of photoinduced surface-active centers is occasioned by the limited range of variation of the latter parameter. Moreover, because of the recombination through defects, the concentration of photoinduced surface-active centers is always smaller than the concentration of

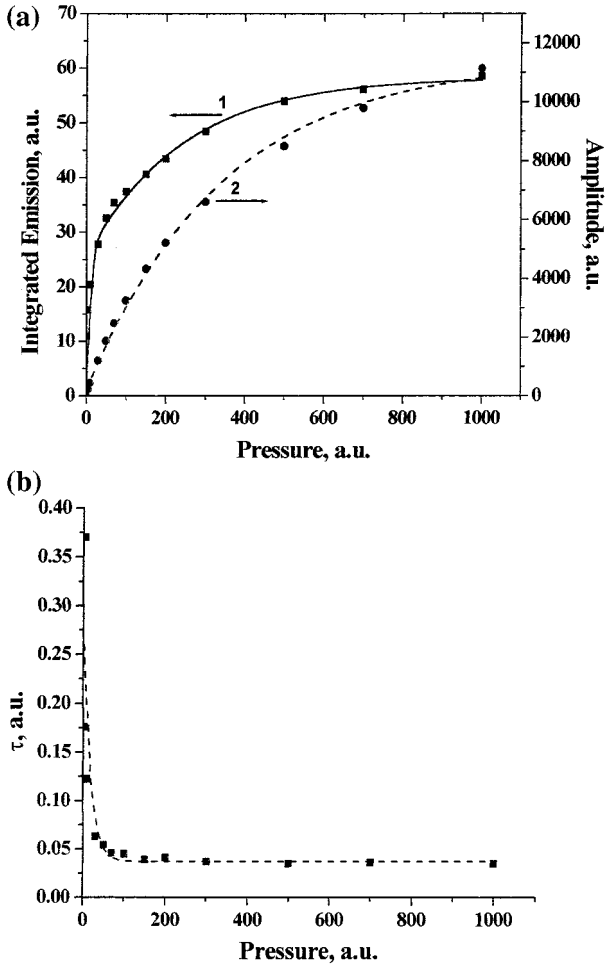

Figure 12. (a) Modeled pressure dependencies of the integrated emission (1) and emission amplitude (2) of the PhICL luminescence on the initial gas pressure. (b) Modeled pressure dependence of the decay time of the PhICL emission on the initial gas pressure.

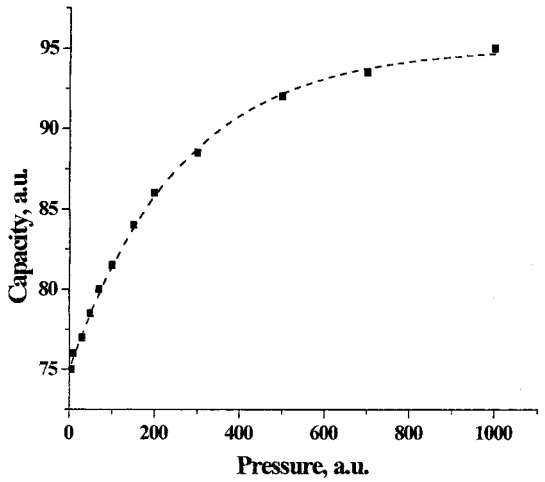

Figure 13. Modeled pressure dependence of the "ultimate adsorption capacity" ($\Delta P_{(t\to\infty)}$) of the photoadsorbent zirconia on the initial gas pressure.

SCHEME 1

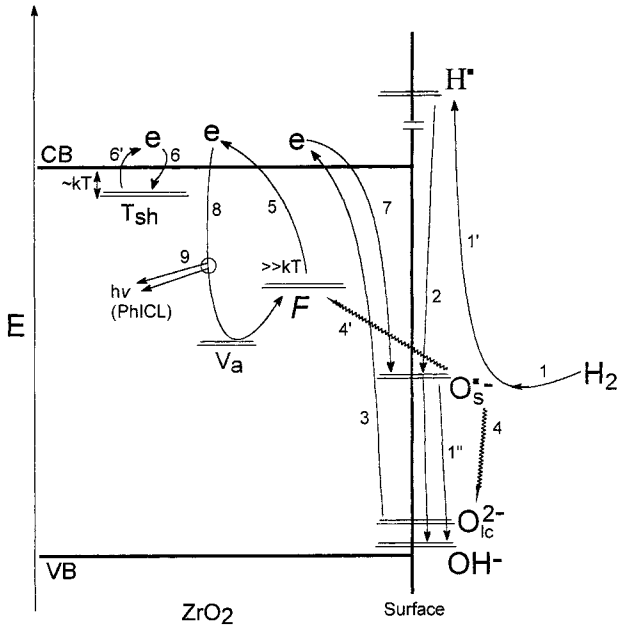

preexisting defects. As a result, the uppermost limit of the concentration of these centers is always low with respect to the concentration (pressure) of another reagent, that is hydrogen, at the pressures used in our experiments. Evidently, other processes are also likely to take place, particularly those described by stages iv, vi, and ix. However, note that the kinetics of both the adsorption of hydrogen on zirconia and the PhICL emission are determined by the limiting step of the hydrogen adsorption on the surface-active $O_s^{-\bullet}$ centers, because the remaining steps, that is, reactions with radicals and electronic processes, tend to be inherently faster.

Consideration of additional reactions of radicals and/or electronic processes will no doubt affect the parameters quantitatively but will not markedly affect the qualitative behavior of the system. To the extent that parameters such as surface adsorption capacity and concentration of photogenerated surface-active centers (among others) remain experimentally elusive, a more complete simulation of the experimental results to a given model must await further experiments and considerations. As well, we are unaware of any experimental evidence for the possible generation and involvement of holes in such adsorption processes for their inclusion in the simulations.

Concluding Remarks

Despite the experimental problems alluded to above, some conclusions can be reached regarding some of the steps in the PhICL process, and this even with our present level of understanding. These steps are summarized in the form presented in Scheme 1. Photoexcitation of a solid (e.g., zirconia) at the appropriate energy leads to light energy conversion and storage by the photogeneration of defects on the solid (e.g., the color centers **F**, $O_s^{-\bullet}$, and others). In addition, the surface states themselves (such as for example the low-coordinated oxide ions, O_{lc}^{2-}) are significant defects with respect to the solid bulk. They are also poised to participate in relaxation processes.

Step 1 in Scheme 1 represents the dissociative chemisorption of hydrogen molecules on photogenerated surface-active hole centers. This leads, in part, to the relaxed state of the surface OH^- group (step 1″) and to the formation of highly energetic hydrogen atoms $H^\bullet$ (step 1′). Step 2 describes the chemical reactions of atomic hydrogen with the surface defects $O_s^{-\bullet}$ and/or O_{lc}^{2-} yielding a chemical pathway for the system to relax. This is subsequently accompanied by the release of energy (step 4) and/or by the generation of free electrons (step 3), which trigger the physical pathway of system relaxation. Energy transfer to the solid electronic subsystem (step 4) also leads to the generation of free electrons (step 5) by detrapping these electrons from the deep energy **F** centers. The fate of these electrons is determined by the physical relaxation processes in the solid, for example, trapping by and detrapping from the shallow traps (steps 6 and 6′). The latter steps are those that are responsible for the temperature dependencies of the PhICL emission, for the recombination with hole states on the zirconia surface (step 7) and in the bulk (not shown) and for the trapping by deep energy electrons traps (step 8) to induce the PhICL emission (step 9).

As evidenced by the experimental results and the simulation presented in this study, there exists another type of interrelationship between the chemical and physical processes in a heterogeneous system. Chemical reactions can cause the release of energy that was stored during the preirradiation of the solid owing to the photoinduced formation of metastable solid defects, such as $O_s^{-\bullet}$, and deep electron traps, which lead to both chemical and physical relaxation of the system. In particular, the latter relaxation mechanism is manifested as a PhICL emission triggered by the adsorption of such donor molecules as hydrogen. As a result of this spontaneous process, the prephotoexcited system decays to a lower energy state.

Acknowledgment. We are grateful to the Natural Sciences and Engineering Research Council of Canada for their kind support of our work (to N.S.).

Appendix: Summary Description of Symbols

α = rate of linear increase of the temperature

D = ionized state of a preexisting defect (without electron)

D^- = preexisting defect with trapped electron

$d[\mathbf{F}]/dt$ = rates of electron trapping by defect sites such as anion (V_a) vacancies

$d[V]/dt$ = rates of hole trapping by defect sites such as cation (V_c) vacancies

dP/dt = rate of gas pressure evolution in a closed reactor

E_G = band gap in the semiconductor electron energy structure

E_{phys} = binding energy of physisorption (energy of desorption)

ΔE = energy released during the dissociative adsorption of hydrogen

$[e^-]$ = concentration of electrons

$[h^+]$ = concentration of holes

$n_i^2 = [e^-][h^+]$ = where n_i is a parameter, which in intrinsic semiconductors is equal to the concentration of carriers (either electrons or holes)

F_e = quasi-Fermi level for electrons in a photoexcited semiconductor

F_h = quasi-Fermi level for holes in a photoexcited semiconductor

$\Delta F = F_e - F_h$ = difference between the two quasi-Fermi levels

[**F**] = concentration of electron centers such as **F**-type centers (such as for example, $\mathbf{F}^+$ and **F** centers) and Zr^{3+}

I_{em} = intensity of the potoinduced chesorluminescence (PhICL) emission

$k_{des} = k^\circ_{des} \exp(-E_{phys}/\kappa T)$ rate constant for the desorption process

$k_{ads} = k^{\circ}_{ads} \exp(-E_a/\kappa T)$ = rate constant for the adsorption process {i.e., reaction rate constant of the chemical interaction between hydrogen (or methane) molecules and surface-active centers}

k_i = rate constants of the corresponding stage i = i−x

N_C = density of electronic states in the conduction band

N_V = density of electronic states in the valence band

$O_s^{-\bullet}$ = photoinduced surface-active center for the adsorption of hydrogen and methane

$\Delta P_{(t\to\infty)}$ = ultimate adsorption capacity of the pre-excited zirconia surface

r_i = rates of the corresponding stage i = i−x

r_{ox} = rates of oxidative chemical processes taking place at the surface

r_{red} = rates of reductive chemical processes taking place at the surface

T_{sh} = empty shallow electron trap

T_{sh}^- = shallow electron trap with trapped electron

[**V**] = concentration of hole centers such as **V**-type centers

V_c = cation vacancy

V_a = anion vacancy

References and Notes

(1) Serpone, N., Pelizzetti, E., Eds.; *Photocatalysis—Fundamentals and Applications*; John Wiley & Sons: New York; 1989.

(2) Baru, V. G.; Volkenstein, Th. Th. *The effect of irradiation on surface properties of semiconductors*; Nauka: Moscow, Russia, 1978.

(3) Fox, M. A.; Dulay, M. T. *Chem. Rev.* **1993**, *93*, 341.

(4) Kamat, P. V. *Chem. Rev.* **1993**, *93*, 267.

(5) Ryabchuk, V. K.; Burukina, G. V. *Sov. J. Phys. Chem.* **1991**, *65*, 1621.

(6) Emeline, A. V.; Ryabchuk, V. K.; Salinaro, A.; Serpone, N. *Int. J. Photoenergy* **2001**, *3*, 1.

(7) Bonch-Bruevich, V. L.; Kalashnikov, S. G. *Physics of Semiconductors*; Nauka: Moscow, Russia, 1990.

(8) Emeline, A. V.; Kataeva, G. V.; Litke, A. S.; Rudakova, A. V.; Ryabchuk, V. K.; Serpone, N. *Langmuir* **1998**, *14*, 5011.

(9) Emeline, A. V.; Petrova, S. V.; Ryabchuk, V. K.; Serpone, N. *Chem. Mater.* **1998**, *10*, 3484.

(10) Andreev, N. S.; Kotel′nikov, V. A. *Kinet. Katal.* **1974**, *15*, 1612.

(11) Emeline, A. V.; Ryabchuk, V. K. *Russ. J. Phys. Chem.* **1998**, *72*, 432.

(12) Andreev, N. S.; Emeline, A. V.; Khudnev, V. A.; Polikhova, S. A.; Ryabchuk, V. K.; Serpone, N. *Chem. Phys. Lett.* **2000**, *325*, 288.

(13) Kotel′nikov, V. A.; Basov, L. L.; Solonitsyn, Yu. P.; Kuzmin, G. N. Institute of Physics, St. Petersburg State University, St. Petersburg, Russia, unpublished data and personal communication to A. Emeline.

(14) Llopis, J. *Phys. Stat. Sol. A* **1990**, *119*, 661.

(15) Michkailov, M. M. *Russ. J. Appl. Spectrosc.* **1984**, *41*, 58.

(16) Purevdorj, D. Ph.D. Thesis, St. Petersburg State University, St. Petersburg, Russia, 1996.

(17) Emeline, A. V.; Kuzmin, G. N.; Purevdorj, D.; Shenderovich, I. G. *Kinet. Katal.* **1997**, *38*, 446.

(18) Che, M.; Tench, A. J. *Adv. Catal.* **1982**, *31*, 77.

(19) Basov, L. L.; Kuzmin, G. N.; Prudnikov, I. M.; Solonitzyn, Yu. P. In *Uspekhi Photoniki.*; Vilesov, Th. I., Ed.; LGU (Leningrad State University): Leningrad, Russia, 1977; Vol. 6, p 82.

(20) Emeline, A. V.; Rudakova, A. V.; Ryabchuk, V. K.; Serpone, N. *J. Phys. Chem. B* **1998**, *102*, 10906.